available at www.sciencedirect.com

ScienceDirect

www.elsevier.com/locate/brainres

BRAIN RESEARCH

Research Report

Glucose transporter 5 is undetectable in outer hair cells and does not contribute to cochlear amplification

Xudong Wu[a], *Xiang Wang*[b], *Jiangang Gao*[a], *Yiling Yu*[a], *Shuping Jia*[b], *Jing Zheng*[c], *Peter Dallos*[c], *David Z.Z. He*[b], *MaryAnn Cheatham*[c], *Jian Zuo*[a,*]

[a]*Department of Developmental Neurobiology, St. Jude Children's Research Hospital, Memphis, TN 38105, USA*
[b]*Department of Biomedical Sciences, Creighton University, Omaha, NE 68178, USA*
[c]*Department of Communication Sciences and Disorders, Northwestern University, Evanston, IL 60208, USA*

ARTICLE INFO

Article history:
Accepted 24 February 2008
Available online 18 March 2008

Keywords:
Hair cell
Cochlear amplification
Glucose transporter
Prestin
Electromotility
Knockout mice

ABSTRACT

Glucose transporter 5 (Glut5) is a high-affinity fructose transporter. It was proposed to be a motor protein or part of the motor complex required for cochlear amplification in outer hair cells (OHCs). Here we show that, in contrast to previous reports, Glut5 is undetectable, and possibly absent, in OHCs harvested from wildtype mice. Further, Glut5-deficient mice display normal OHC morphology and motor function (i.e., nonlinear capacitance and electromotility) and normal cochlear sensitivity and frequency selectivity. We conclude that Glut5 is not required for OHC motility or cochlear amplification.

1. Introduction

Cochlear outer hair cells (OHCs) elongate and contract in response to changes in their membrane potential (Brownell et al., 1985), and are thus able to feed energy back to the basilar membrane. This feature of OHCs, termed electromotility, has been proposed to form the cellular basis of the cochlear amplifier, an active mechanical amplification mechanism in the cochlea (Dallos, 1992; Davis, 1983). Associated with OHC electromotility is a nonlinear capacitance (NLC) derived from voltage-dependent charge movement within motor proteins in the cell's lateral membrane (Ashmore, 1989; Santos-Sacchi, 1991). A high density of protein particles has also been observed in the plasma membrane of OHCs (Forge, 1991; Gulley and Reese, 1977; Kalinec et al., 1992) and it is assumed that these protein particles constitute the cellular motor (Kalinec et al., 1992; Santos-Sacchi and Navarrete, 2002).

Glucose transporter 5 (Glut5 or Slc2a5) has been proposed to be the motor protein or part of the motor complex of OHCs and thus required for cochlear amplification (Ashmore et al., 2000; Geleoc et al., 1999). This proposal is based on the knowledge that fructose can affect the NLC and electromotility of OHCs (Geleoc et al., 1999). Moreover, Glut5 is the only high-affinity fructose transporter detected along the lateral wall of OHCs using immunostaining (Ashmore et al., 2000; Belyantseva et al., 2000; Geleoc et al., 1999; Nakazawa et al., 1995). It is also abundantly expressed in the epithelial brush border of the small intestine, S3 proximal tubules of kidney, and in the

* *Corresponding author*. Fax: +1 901 495 2270.
E-mail address: jian.zuo@stjude.org (J. Zuo).

Abbreviations: Glut5, Glucose transporter 5; OHCs, outer hair cells; NLC, nonlinear capacitance; TEM, transmission electron microscopy; ABR, Auditory brainstem response; LCM, laser-capture microscopy; CAP, compound action potential

0006-8993/$ – see front matter © 2008 Elsevier B.V. All rights reserved.
doi:10.1016/j.brainres.2008.02.094

sperm of the testis and epididymis (Angulo et al., 1998; Burant et al., 1992; Miyamoto et al., 1994; Sugawara-Yokoo et al., 1999).

Discovery of a novel gene *prestin* has rendered Glut5 a less promising candidate (Zheng et al., 2000). Prestin is highly expressed in the lateral membrane of the OHCs and is required for OHC electromotility and NLC and for cochlear amplification in vivo (Adler et al., 2003; Liberman et al., 2002; Zheng et al., 2000). It is also known that the Glut5 immunosignal during postnatal development is detected after the expression of prestin in OHCs and after the first occurrence of electromotility (Belyantseva et al., 2000). Moreover, co-expression of Glut5 with prestin in Chinese Hamster Ovary (CHO) cells does not alter prestin-mediated NLC (Ludwig et al., 2001). Recently, it was also demonstrated that prestin and Glut5 interact in HEK293T cells although the precise subcellular sites of such interactions remain unclear (Wu et al., 2007). Hence, the exact roles of Glut5 in OHC electromotility and NLC and in cochlear amplification remain unclear.

Here we report on the generation and characterization of Glut5 knockout mice. Surprisingly, we find that Glut5 is absent or undetectable in wildtype OHCs, which differs from previous reports. Results provide evidence that Glut5 is not required for OHC electromotility or for cochlear amplification.

2. Results

2.1. *Generation of Glut5 floxed and null mice*

To make a *Glut5*^{floxed} mouse model, we inserted one loxP site upstream of the predicted promoter and exon 1 and another loxP site downstream of exon 4 of the *Glut5* gene which has 14 exons (Fig. 1A). Theoretically, Cre activity can cause the deletion of a total of 6.6 kb genomic DNA that contains: 1) the predicted promoter located upstream of exon1 by GeneScan; 2) the ATG translation initiation codon in exon 3; and 3) the N-terminal 43 amino acids including the first transmembrane domain.

A Southern blot screen showed that 14 among 160 ES clones picked had undergone homologous recombination. Two of the positive ES clones with normal karyotype were used for blastocyst injection. High chimeric mice from either clone were crossed with C57BL6/J mice to achieve F1 germline transmitted heterozygous mice that carried the *Glut5*^{floxed} allele.

Intercrosses between *Glut5*$^{floxed/+}$ and a ubiquitous Cre expressing line EIIA-Cre (Lakso et al., 1996) resulted in offspring with the expected deletion of the floxed exons 1–4 of *Glut5*

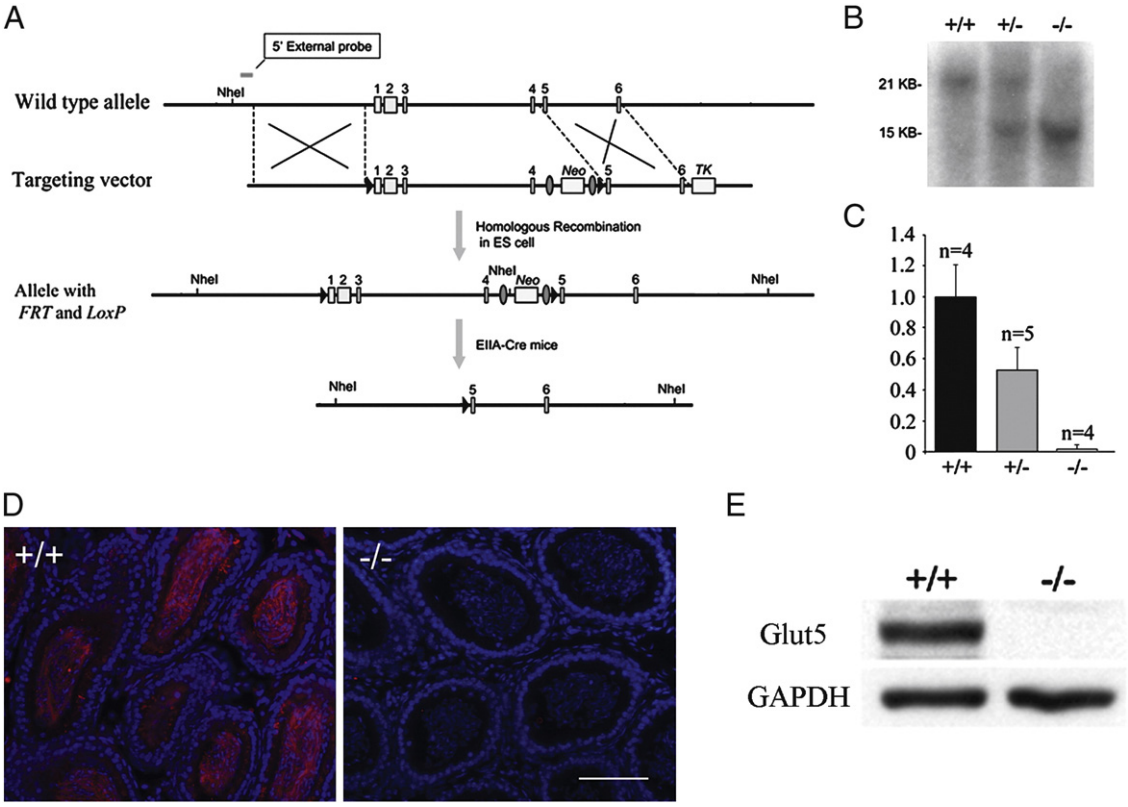

Fig. 1 – Targeted disruption of the Glut5 gene and distribution of Glut5 in cochleae, testis and epididymis. (A) Strategy for targeted deletion of the *Glut5* gene. TK, thymidine kinase gene. (B) Tail genomic Southerns (digested with NheI) from wildtype (+/+), *Glut5* heterozygous (+/–) and *Glut5* homozygous (–/–) N1F3 mice after the floxed *Glut5* portion was deleted by crossing with EIIA-Cre mice. (C) Real-time RT-PCR analysis of cochlear Glut5 mRNA levels in wildtype (+/+), heterozygous (+/–), and homozygous (–/–) mice at P9. *Y* axis: relative ratio. Bars: S.E.M. *n*: the number of mice used in each genotype. Similar results were obtained in kidney. (D) Immunostaining of Glut5 in epididymis of wildtype and *Glut5*–/– mice. Glut5: red; DAPI: blue. Bar=80 μm. Similar results were obtained in epididymis. (E) Western analysis of Glut5 in testis. Gapdh is used as a loading control.

(namely the *Glut5*$^{del1–4}$ allele) (Fig. 1B). Because the *Glut5*$^{del1–4}$ allele was subsequently maintained and analyzed in the absence of EIIA-Cre, the deletion of floxed exons 1–4 of *Glut5* was indeed transmitted germline.

As expected, no *Glut5* transcript was detected in the cochlea or the kidney of *Glut5*$^{del1–4/del1–4}$ mice whereas the mRNA levels in cochlea and kidney from *Glut5*$^{del1–4/+}$ mice were approximately 0.51 and 0.38 fold, respectively, of those from wildtype littermates (Fig. 1C and data not shown).

It was reported that two splicing variances of Glut5 mRNA exist in mouse (Corpe et al., 2002). Both splicing variances occur upstream of the ATG start codon in exon 3 according to the updated genomic sequence from www.ensembl.org (Corpe et al., 2002). Thus, both splicing forms of Glut5 mRNA will be deleted with the 5′ untranslated region, the ATG start codon, and the first 43 amino acids of the coding sequence by our knockout strategy. Fig. 1 also shows results of immunostaining and Western blots using the anti-mouse Glut5-C terminal antibody (Wu et al., 2007). In wildtype mice, Glut5 was highly expressed in the sperm of testis and epididymis but no Glut5 was detected from either testis or epididymis in *Glut5*$^{del1–4/del1–4}$ mice (Fig. 1D). Similar results were obtained using Western blot analysis of the testis (Fig. 1E). These results indicate that the remaining 3′ coding part of GLUT5 gene does not generate a truncated Glut5 protein. Glut5 protein was, therefore, successfully deleted in *Glut5*$^{del1–4/del1–4}$ mice, i.e., *Glut5*$^{del1–4/del1–4}$ mice are *Glut5*-null or *Glut5*–/–.

2.2. *Expression of Glut5 in OHCs*

Because of the presence of Glut5 mRNA in the wildtype whole cochleae (Fig. 1C) and previous reports of the presence of Glut5 protein in the OHC's lateral wall (Belyantseva et al., 2000; Geleoc et al., 1999), we extensively examined whether Glut5 protein is present in mouse OHCs. We first performed immunostaining using the same antibody (anti-huGLUT5-C antibody, #4670–1756, Biogenesis, Brentwood, NH, or catalog #AB1048, Chemicon, Temecula, CA) reported to detect the positive signal along the lateral wall of OHCs from rat and mouse (Belyantseva et al., 2000; Geleoc et al., 1999). In our hands (both Zuo and Dallos labs), this antibody indeed stained the OHC's lateral wall in wildtype mice but surprisingly did not stain OHCs in prestin knockout mice (Wu et al., 2003). However, this antibody did not label sperm in wildtype mouse testis sections, a well-known positive control for Glut5 (data not shown). Indeed, this antibody was known not to react with rodent Glut5 (Biogenesis data sheet). Furthermore, after 2005, the new batches of antibody with the same catalog number (Biogenesis) and likely derived from a new rabbit, did not label the lateral wall of wildtype OHCs or sperm (data not shown). Therefore, the signal in the OHC's lateral wall detected by this anti-human GLUT5 antibody is likely a cross-reaction with some unknown protein(s) but not Glut5. Why its signal is lost in prestin knockout OHCs remains a mystery. Furthermore, using our custom-made anti-mouse Glut5-C antibody (Wu et al., 2007) and the anti-rat Glut5-N antibody (SC-14844), we found no significant differences between wildtype and knockout mice and no signals in OHCs (Fig. 2A).

To definitively determine if Glut5 mRNA is present in OHCs, we also performed RT-PCR analysis from isolated wildtype mouse OHCs by using laser-capture microscopy (LCM) (Gao et al., 2007a) and from a mouse OHC cDNA pool made by using the LCM method (Anderson and Zheng, 2007). Both analyses yielded negative results in OHCs, although a Glut5 message is detected in the whole cochlear cDNA (Fig. 2B). Because three pairs of primers from three different

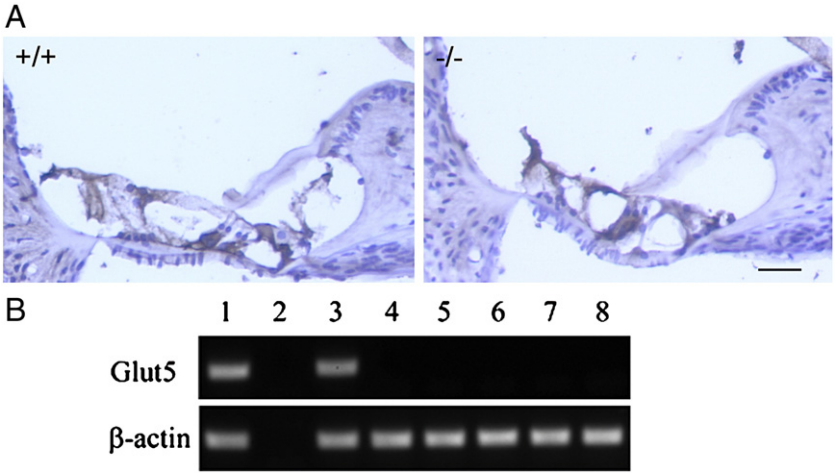

Fig. 2 – Expression of Glut5 in cochleae. (A) Immunostaining of cochlear sections using the custom-made anti-mouse Glut5-C antibody. No significant differences were observed between wildtype and Glut5–/– mice. Both cochlear sections show similar background staining in some cell types, which suggests some cross reactivity. Identical background staining was observed between both genotypes using different secondary antibodies and antigen-retrieval procedures (data not shown). Bar = 40 μm. (B) RT-PCR analysis of laser-captured OHCs and other cells in the wildtype mouse cochlear sections (see controls for other cell-type specific markers which were performed on same batches of cochlear sections as in (Gao et al., 2007a). Lane 1: Positive control of cDNA from P9 whole cochleae as the template. Lane 2: Negative control of mRNA of P9 whole cochleae without reverse transcription as the template. Lane 3: All cells scraped from cochlear sections. Lanes 4–8: Laser-captured (LC) cell types from cochlear sections: 4. inner hair cells; 5. outer hair cells; 6. Deiters cells; 7. Claudius cells; and 8. spiral ganglia.

regions of Glut5 cDNA were used in these analyses, cochlea-specific alternative splicing in addition to the two known splicing forms is unlikely (Corpe et al., 2002).

2.3. *Morphological analysis of Glut5−/− cochleae*

The *Glut5*−/− mice appeared to behave normally and have normal body weight. For analysis of *Glut5*−/− cochlear morphology, we evaluated plastic sections stained with toluidine blue and paraffin sections with H&E staining. No obvious defects were found in *Glut5*−/− cochleae (data not shown). Detailed subcellular structures of the lateral wall of OHCs were further examined using transmission electronic microscopy (Fig. 3A). In the lateral wall of OHCs from *Glut5*−/− mice, the plasma membrane exhibited the typical wavy surface observed in wildtype OHCs: one layer of subsurface cisternae (SSC) and no apparent abnormalities (Wu et al., 2004). In addition, a row of evenly distributed dots, presumably the pillars connect subsurface cisternae and plasma membrane in homozygotes. These results indicate that the tri-laminar structure appeared intact in *Glut5*−/− OHCs.

To determine if prestin was affected by the disruption of Glut5, immunostaining using a prestin C-terminus antibody was performed on the *Glut5*−/− cochlear sections and whole-mount basilar membrane specimens at P28 (Fig. 3B). The prestin signal appeared in the lateral wall of OHCs in *Glut5*−/− mice and no significant hair cell loss was observed in *Glut5*−/− cochleae (data not shown). In addition, myosin7a and myosin1c, the two hair-bundle related motor proteins, and synaptophysin, a synaptic marker of OHCs, were also present in *Glut5*−/− mice (immunostaining data not shown).

We also examined potential defects in the glycogen content of OHCs in Glut5−/− mice. However, no significant differences were observed between wildtype and Glut5−/− OHCs (data not shown) (Ding et al., 1999).

2.4. *Electromotility and NLC of isolated Glut5−/− OHCs*

To ascertain whether the electromotility and NLC of OHCs isolated from *Glut5*−/− mice were affected, we directly measured both electromotility and NLC in isolated OHCs from wildtype and *Glut5*−/− mice (Fig. 4). The cell lengths of wildtype and *Glut5*−/− OHCs at −70 mV holding potential for motility measurements were 27.4±1.5 μm (n=9) and 25.4±1.3 μm (n=7). We compared the magnitude of maximal motile response (saturated response) at the membrane potentials of −100 and +60 mV. The motility magnitude of wildtype and *Glut5*−/− OHCs was 955.7±284.6 nm (n=9) and 1150.8±291.9 nm (n=7). A Student's t-test showed that no significant differences existed between wildtype and *Glut5*−/− OHC motility magnitudes (p=0.2). Moreover, *Glut5*−/− OHCs (n=7) displayed wildtype-like (n=9) NLC: for wildtype vs *Glut5*−/−, Qmax=968.9±118.5 vs 936.2±191.5 fC, alpha=30.9±3.7 vs 31.4±2.3 mV, Vpkcm=−54.2±11.5 vs −50.7±14.0 mV, charge density=127.9±10.6 vs 125.2±40.5 fC/pF. Student's t-tests showed no significant differences between wildtype (n=9) and *Glut5*−/− (n=7) OHC (Qmax: p=0.65, alpha: p=0.72, Vpkcm: p=0.58, charge density: p=0.85).

2.5. *Cochlear physiology*

We further characterized *Glut5*−/− mice between 1 and 2 months of age by measuring thresholds, input–output

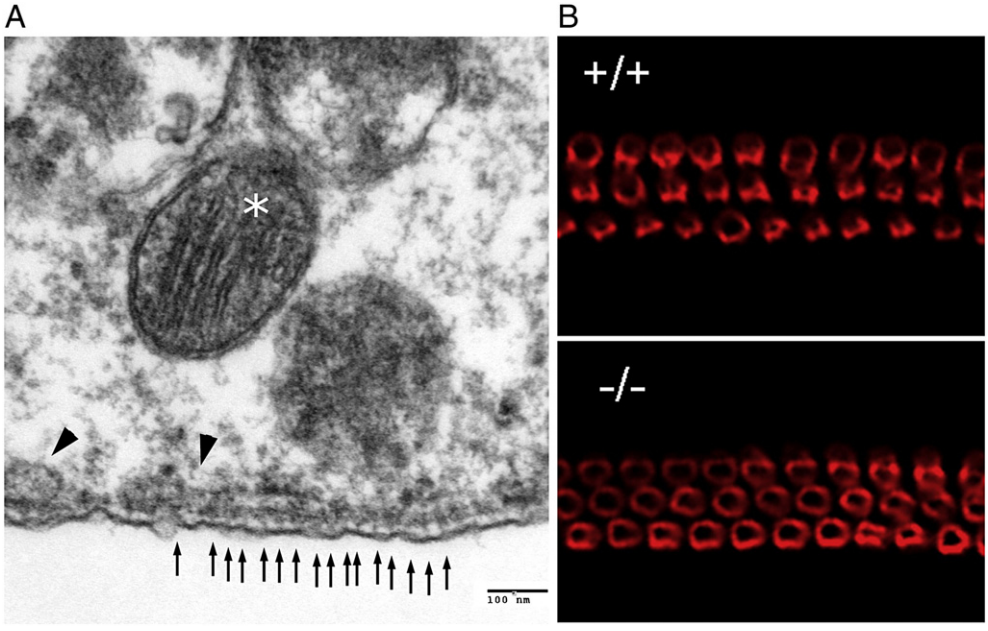

Fig. 3 – (A) Normal tri-laminar structure in the lateral walls of *Glut5*−/− mice. A row of evenly distributed dots (small arrows), most likely the pillars, is found along the lateral wall in OHCs of *Glut5*−/− mice. One layer of SSC (arrow heads) is located inside the wavy plasma membrane. In addition, many mitochondria (asterisk) are also positioned in the cytoplasm close to the lateral wall. (B) Prestin immunostaining in whole-mount preparations from the basal turns of wildtype and Glut5−/− mice. Deletion of Glut5 does not affect the targeting of prestin to the OHC lateral wall.

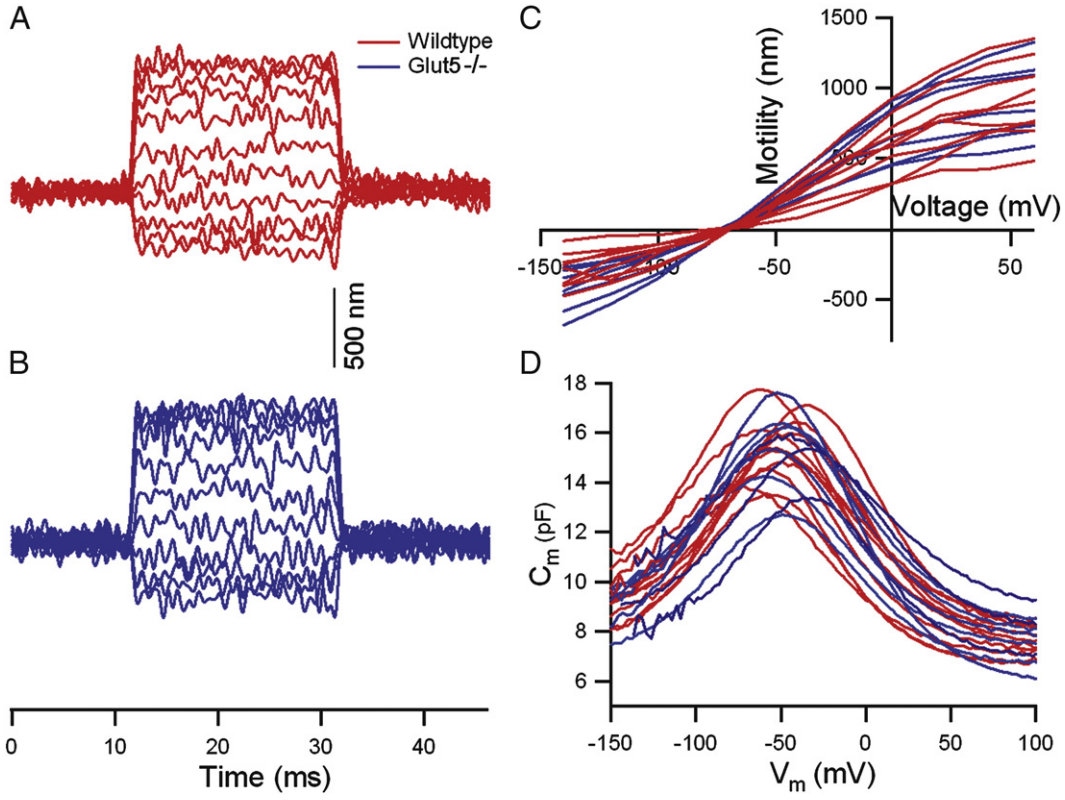

Fig. 4 – Motility and NLC measured from +/+ and *Glut5*–/– OHCs in vitro. (A, B) Representative examples of electromotility from +/+ (red) and *Glut5*–/– (blue) OHCs measured when the membrane potential was stepped from a holding potential of –70 mV to different values (from –140 to 60 mV) at 20-mV increments. Contraction is plotted upward. (C) Individual motility functions obtained from +/+ (red) and *Glut5*–/– (blue) OHCs. (D) Individual NLC curves (+/+ in red, *Glut5*–/– in blue) measured using the two-sine voltage stimulus protocol (10 mV peak at 390.6 and 781.2 Hz) with subsequent fast Fourier transform-based admittance analysis.

functions and tone-on-tone masking tuning curves for the compound action potential (CAP) (Fig. 5) (Cheatham et al., 2004; Gao et al., 2007b). No changes in sensitivity, tuning or input-output relationships were detected in *Glut5*–/– mice when compared to wildtype controls. Auditory brainstem response (ABR) thresholds with click, 4, 8, 16, and 32 kHz stimuli were also similar between *Glut5*–/– and wildtype mice at P28 (data not shown).

3. Discussion

In our characterization of Glut5–/– mice, we discovered that the lack of Glut5 did not alter cochlear morphology, OHC electromotility or NLC. After measuring various indices of peripheral and central auditory physiology (i.e., ABR and CAP), we also demonstrated that the lack of Glut5 did not change cochlear amplification or tuning. At the morphological level, no apparent abnormality was observed in the cochleae of *Glut5*–/– mice. Immunostaining showed normal expression of prestin, myosin1c, myosin7a, and synaptophysin. TEM analysis (Fig. 3) also displayed the regular tri-laminar structure in the lateral wall of OHCs.

Given that we could not definitively demonstrate, despite numerous attempts with various antibodies, that Glut5 is present in wildtype OHCs, and that no Glut5 mRNA was detected in our two sensitive OHC RT-PCR methods, we conclude that Glut5 is either not expressed, or expressed at undetectable levels. Immunostaining results in previous publications were obtained using a commercial antibody raised against a human GLUT5-C terminal peptide. It is now known that this antibody does not stain sperm in mice, and does not react with rodent tissues. More importantly, the experiments lacked the most appropriate negative controls, i.e., Glut5–/– mice. Hence, it remains possible that the human antibody recognized a Glut5-like epitope as suggested initially (Geleoc et al., 1999) and that such an epitope was missing in prestin knockout mouse OHCs. Unfortunately, this original antibody is now unavailable, making further tests impossible.

In support, we found that Glut5 is absent in all accessible cDNA libraries constructed from various tissues (inner ear, cochlea, otocyst, organ of Corti, or hair cells) from several species including mouse and analyzed by various groups (dbEST ID: 18222; 9974; 11139; 10920; 4088; 14415; 16641) (Beisel et al., 2004; Klockars et al., 2003; McDermott et al., 2007; Peters et al., 2007; Pompeia et al., 2004; Robertson et al., 1994; Roche

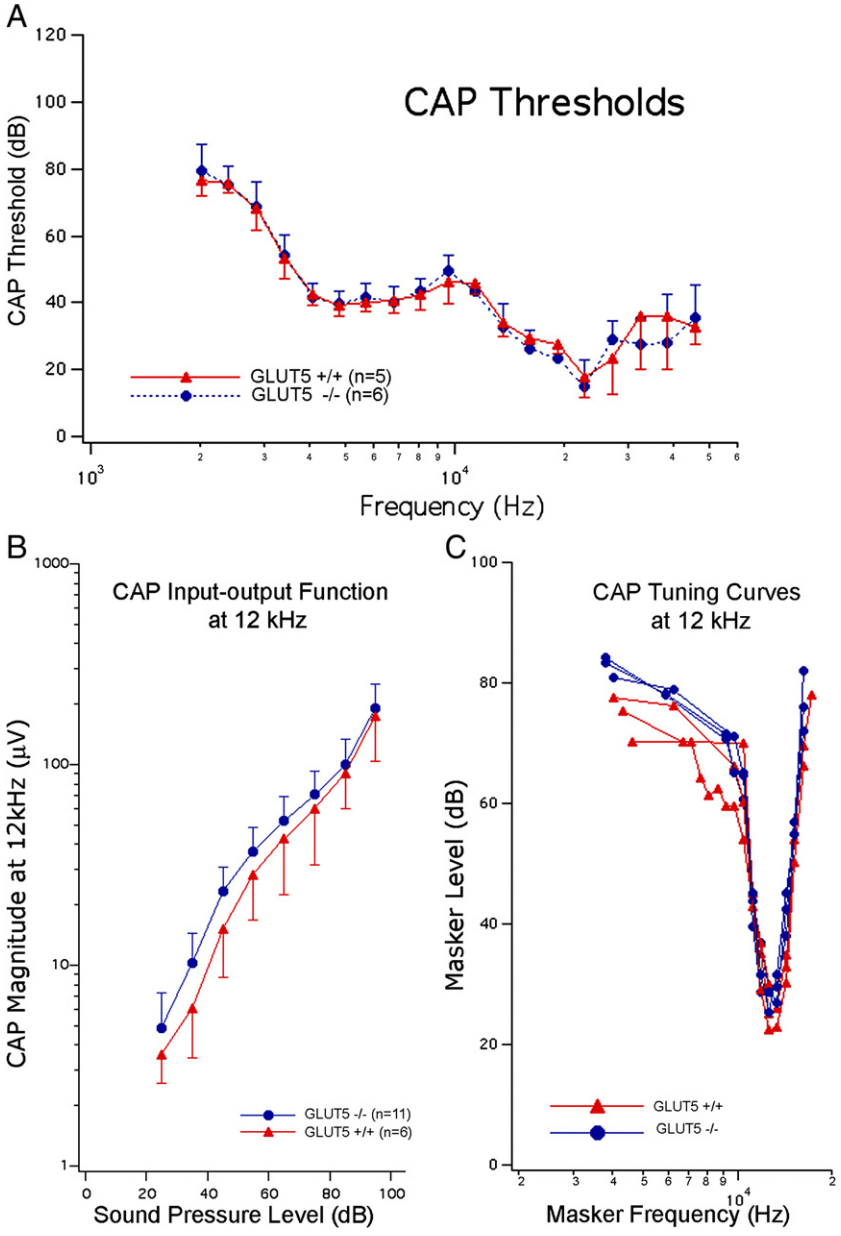

Fig. 5 – In vivo cochlear physiology of *Glut5*–/– mice. All measurements were obtained from +/+ (red) and *Glut5*–/– (blue) mice at 1–2 months of age. Bars represent standard deviations. (A) Mean CAP thresholds. (B) Mean CAP input–output functions at 12 kHz. (C) CAP tuning curves at 12 kHz obtained using simultaneous masking.

et al., 2005; Zheng et al., 2000). Based on cochlear RT-PCR results, however, Glut5 mRNA is present in other cochlear cells of wildtype mice, although the cochlear cDNA used could have been contaminated with blood cells. Hence, a functional Glut5 could still be present in OHCs with a long half-life and extremely low mRNA level. Therefore, it is possible that interactions between prestin and Glut5 in transfected 293 cells occurred predominantly in subcellular compartments during protein maturation and sorting, rather than at the plasma membrane (Wu et al., 2007). In addition, it is possible that the interaction between Glut5 and prestin only exists when they are both over-expressed in a heterologous system. A possible role of Glut5 in the metabolism of OHCs requires further study. Regardless, our results in *Glut5*–/– mice demonstrate that this transporter is not required for normal OHC electromotility and cochlear amplification in vivo.

4. Experimental procedures

4.1. *The floxed Glut5 targeting construct*

Three BAC clones (C466F17, C87K12, and C83I21, Invitrogen) were identified containing the *Glut5* gene in RPCI22 mouse BAC high-density membranes. A 14.4 kb *Glut5* genomic fragment was retrieved from the BAC clone to make the targeting vector as described previously (Gao et al., 2007b). The targeting vector for the floxed *Glut5* was finalized

after the FRT-neo-FRT-loxP cassette was inserted into the plasmid.

4.2. *Embryonic stem (ES) cells*

Linearized targeting vector was electroporated into 129/SvEv (129S6) ES cells. The ES cell clones were screened by Southern blot using an external probe and primers G5 EP 3903 (5′-GAG CAA GCT GGT CAT GCA TCT) and G5EP 4153 (5′-CCA GTG CTC ACC CAA CGT TT), which detected a 19 kb band for the wild-type allele and a 6 kb band for the floxed allele.

4.3. *Germline transmission*

High chimera mice generated from blastocyte injection were crossed with C57BL6/J and both lines (E7 and A11) went through germline. F1 mice carrying the floxed *Glut5* allele were then either intercrossed or crossed with EIIA-Cre mice. To eliminate the EIIA-Cre mosaic effect, we chose germline transmitted knockout mice that were negative for Cre in the N1F3 and N1F4 generations. The primers used for genotyping are listed as follows: G5 Flox 931F (5′-GCT GTG CTC GAC GTT GTC AC) and G5 Flox 1431 R (5′-ACC GTA AAG CAC GAG GAA GC) for the floxed allele; G5 KO-69F (5′-GTT GGT CGC GTT GAA CTG C) and G5 KO-271R (5′-AGG GCA CAG ACC GAC AGA AC) for the deleted *Glut5* allele; G5 geno F (5′-GGC AGT GTG TGG AGT CAT CG) and G5 geno R (5′-GGG AAC ATG GAC ACC GTC AG) for wildtype allele; and Cre F (5′-TGC AAC GAG TGA TGA GGT TC) and Cre R (5′-ACG AAC CTG GTC GAA ATC AG) for the Cre allele.

4.4. *RNA purification and real-time RT-PCR*

Tissue RNA was prepared with Omniscript Reverse Transcriptase as described previously (Liberman et al., 2002). For real-time PCR, specific primers and probe covering exons 9~10 of the *Glut5* cDNA (G5 taq 668F: 5′-TGC TGA TCC AGA AGA AAG ATG AAG; G5 taq 727R: 5′-CGT CTT TCC AGC CTC GGA; G5 taqman probe: 6FAM-AGC TGC TGA GAG AGC CCT CCA GAC C-BOH) were used. Real-time PCR was performed as previously described (Liberman et al., 2002).

4.5. *Laser capture microdissection*

These procedures were described previously (Anderson and Zheng, 2007; Gao et al., 2007a). Laser capture microdissection was performed using the PixCell II system (Arcturus). We employed a method described previously (Pagedar et al., 2006) but with some modifications. Briefly, mice (8 week old) were perfused intracardially with 4% PFA in phosphate buffer. Cochleae were then post-fixed 8 min (Anderson and Zheng, 2007) or overnight, decalcified, embedded in paraffin, and sectioned at 12 μm. We used the Paradise Whole Transcript RT Reagent System (Arcturus, Mountain View, CA) to purify mRNA from both whole cells and laser-captured cells from cochlear sections. The mRNA pool size range was 0.1 to 1.2 kb. For PCR, we designed 1 pair of primers to amplify the cDNA of Glut5 (G5-RT-PCR-F: 5′-AAT GGG CTG CAG CCA AAT TG; and G5-RT-PCR-R: 5′-GAA GGC CAA ACA GCT GGG C) and another pair for β-actin (β-actin-F: 5′-AAT TTC TGA ATG GCC CAG GT and β-actin-R: 5′-TGT GCA CTT TTA TTG GTC TCA A). We used cDNA from whole P9cochleae as a positive control, and mRNA from whole P9 cochleae without reverse transcription as a negative control.

4.6. *ABR recording*

The ABR assay was performed as described previously (Gao et al., 2007b; Wu et al., 2004). Briefly, click and tone pips at 4, 8, 16, and 32 kHz were generated using a Tucker Davis Technologies (TDT, Gainsville, FL) workstation (System III).

4.7. *NLC and electromotility of OHCs*

The OHC electromotility and NLC were measured as described previously (Gao et al., 2007b; Jia and He, 2005).

4.8. *CAP measurements*

Cochlear in vivo physiology was studied in +/+ and *Glut5*–/– mice anaesthetized with sodium pentobarbital (80 mg/kg, IP) as described previously (Cheatham et al., 2004; Dallos and Cheatham, 1976; Gao et al., 2007b).

4.9. *Immunohistochemistry*

Mice were intracardiacally perfused and fixed with 4% PFA. The inner ear was isolated, post-fixed, decalcified, and embedded in paraffin. De-paraffinized sections were routinely treated with 10 mM sodium citrate buffer (pH=6.0) in 85 °C for 15 min for unmasking antigen. Slides were blocked with blocking solution, incubated in primary antibody overnight at 4 °C, rinsed with PBS five times. Slides were then incubated in either Alexa 488-conjugated secondary antibody raised in goat (Molecular Probes, Eugene, OR) or processed with a Vectastain ABC kit according to the product manual (Vector). Fluorescently stained sections were mounted on the slide with the Vectashield mounting media with DAPI (Vector). DAB stained sections were counterstained shortly with hematoxylin.

4.10. *TEM*

Tissues were briefly washed in 0.1 M PBS, post-fixed in 0.8% osmium tetroxide/3% ferrocyanide/0.1 M PBS for 2 h, and washed with deionized, distilled water, then dehydrated through a series of ascending concentrations of ethanol and stained en bloc with 2% uranyl acetate/100% ETOH under a vacuum for 1 h at 60 °C, and embedded in Spurr's resin (Ted Pella), polymerized for 2 days at 60 °C. Ultra-thin sections were cut with a diamond knife, counterstained, and observed by transmission electron microscopy.

4.11. *Western blot*

50 μg of sperm whole cell lysates was subjected to SDS-polyacrylamide gel electrophoresis, followed by blotting onto a polyvinyliden difluoride membrane (Millpore). Because heat may induce the formation of high-molecular-weight membrane protein aggregation, sperm whole cell lysates were not boiled. Primary antibodies used were custom-made anti-mouse Glut5-C terminal antibody (0.5 μg/ml) (Wu et al.,

2007), and anti-GAPDH monoclonal antibody (1:1000 dilution, Chemicon). The membrane was then incubated for 1 h at room temperature with appropriate secondary antibody coupled with horseradish peroxidase. Immunoreactive bands were visualized by ECL detection reagents (GE Healthcare, Piscataway, NJ).

Acknowledgments

This work is supported in part by ALSAC, The Hugh Knowles Center and by NIH grants DC00089 (to P. D.), DC06471, DC05168, DC008800 and CA21765 (to J. Zuo), DC 004696 (to D. Z.Z.H.), and DC006412 (to J. Zheng). J. Zuo is a recipient of a Hartwell Individual Biomedical Research Award.

REFERENCES

Adler, H.J., Belyantseva, I.A., Merritt Jr., R.C., Frolenkov, G.I., Dougherty, G.W., Kachar, B., 2003. Expression of prestin, a membrane motor protein, in the mammalian auditory and vestibular periphery. Hear. Res. 184, 27–40.

Anderson, C.T., Zheng, J., 2007. Isolation of outer hair cells from the cochlear sensory epithelium in whole-mount preparation using laser capture microdissection. J. Neurosci. Methods 162, 229–236.

Angulo, C., Rauch, M.C., Droppelmann, A., Reyes, A.M., Slebe, J.C., Delgado-Lopez, F., Guaiquil, V.H., Vera, J.C., Concha, I.I., 1998. Hexose transporter expression and function in mammalian spermatozoa: cellular localization and transport of hexoses and vitamin C. J. Cell. Biochem. 71, 189–203.

Ashmore, J.F., 1989. Transducer motor coupling in cochlear outer hair cells. In: Wilson, J.P., Kemp, D.T. (Eds.), Cochlear Mechanisms. Plenum Press, London, pp. 107–116.

Ashmore, J.F., Geleoc, G.S., Harbott, L., 2000. Molecular mechanisms of sound amplification in the mammalian cochlea. Proc. Natl. Acad. Sci. U. S. A. 97, 11759–11764.

Beisel, K.W., Shiraki, T., Morris, K.A., Pompeia, C., Kachar, B., Arakawa, T., Bono, H., Kawai, J., Hayashizaki, Y., Carninci, P., 2004. Identification of unique transcripts from a mouse full-length, subtracted inner ear cDNA library. Genomics 83, 1012–1023.

Belyantseva, I.A., Adler, H.J., Curi, R., Frolenkov, G.I., Kachar, B., 2000. Expression and localization of prestin and the sugar transporter GLUT-5 during development of electromotility in cochlear outer hair cells. J. Neurosci. 20, RC116.

Brownell, W.E., Bader, C.R., Bertrand, D., de Ribaupierre, Y., 1985. Evoked mechanical responses of isolated cochlear outer hair cells. Science 227, 194–196.

Burant, C.F., Takeda, J., Brot-Laroche, E., Bell, G.I., Davidson, N.O., 1992. Fructose transporter in human spermatozoa and small intestine is GLUT5. J. Biol. Chem. 267, 14523–14526.

Cheatham, M.A., Huynh, K.H., Gao, J., Zuo, J., Dallos, P., 2004. Cochlear function in Prestin knockout mice. J. Physiol. 560, 821–830.

Corpe, C.P., Bovelander, F.J., Munoz, C.M., Hoekstra, J.H., Simpson, I.A., Kwon, O., Levine, M., Burant, C.F., 2002. Cloning and functional characterization of the mouse fructose transporter, GLUT5. Biochim. Biophys. Acta 1576, 191–197.

Dallos, P., 1992. The active cochlea. J. Neurosci. 12, 4575–4585.

Dallos, P., Cheatham, M.A., 1976. Compound action potential (AP) tuning curves. J. Acoust. Soc. Am. 59, 591–597.

Davis, H., 1983. An active process in cochlear mechanics. Hear. Res. 9, 79–90.

Ding, D.L., McFadden, S.L., Wang, J., Hu, B.H., Salvi, R.J., 1999. Age- and strain-related differences in dehydrogenase activity and glycogen levels in CBA and C57 mouse cochleas. Audiol. Neuro-otol. 4, 55–63.

Forge, A., 1991. Structural features of the lateral walls in mammalian cochlear outer hair cells. Cell Tissue Res. 265, 473–483.

Gao, J., Maison, S.F., Wu, X., Hirose, K., Jones, S.M., Bayazitov, I., Tian, Y., Mittleman, G., Matthews, D.B., Zakharenko, S.S., Liberman, M.C., Zuo, J., 2007a. Orphan glutamate receptor delta1 subunit required for high-frequency hearing. Mol. Cell. Biol. 27, 4500–4512.

Gao, J., Wang, X., Wu, X., Aguinaga, S., Huynh, K., Jia, S., Matsuda, K., Patel, M., Zheng, J., Cheatham, M., He, D.Z., Dallos, P., Zuo, J., 2007b. Prestin-based outer hair cell electromotility in knockin mice does not appear to adjust the operating point of a cilia-based amplifier. Proc. Natl. Acad. Sci. U. S. A. 104, 12542–12547.

Geleoc, G.S., Casalotti, S.O., Forge, A., Ashmore, J.F., 1999. A sugar transporter as a candidate for the outer hair cell motor. Nat. Neurosci. 2, 713–719.

Gulley, R.L., Reese, T.S., 1977. Regional specialization of the hair cell plasmalemma in the organ of corti. Anat. Rec. 189, 109–123.

Jia, S., He, D.Z., 2005. Motility-associated hair-bundle motion in mammalian outer hair cells. Nat. Neurosci. 8, 1028–1034.

Kalinec, F., Holley, M.C., Iwasa, K.H., Lim, D.J., Kachar, B., 1992. A membrane-based force generation mechanism in auditory sensory cells. Proc. Natl. Acad. Sci. U. S. A. 89, 8671–8675.

Klockars, T., Perheentupa, T., Dahl, H.H., 2003. In silico analyses of mouse inner-ear transcripts. J. Assoc. Res. Otolaryngol. 4, 24–40.

Lakso, M., Pichel, J.G., Gorman, J.R., Sauer, B., Okamoto, Y., Lee, E., Alt, F.W., Westphal, H., 1996. Efficient in vivo manipulation of mouse genomic sequences at the zygote stage. Proc. Natl. Acad. Sci. U. S. A. 93, 5860–5865.

Liberman, M.C., Gao, J., He, D.Z., Wu, X., Jia, S., Zuo, J., 2002. Prestin is required for electromotility of the outer hair cell and for the cochlear amplifier. Nature 419, 300–304.

Ludwig, J., Oliver, D., Frank, G., Klocker, N., Gummer, A.W., Fakler, B., 2001. Reciprocal electromechanical properties of rat prestin: the motor molecule from rat outer hair cells. Proc. Natl. Acad. Sci. U. S. A. 98, 4178–4183.

McDermott Jr., B.M., Baucom, J.M., Hudspeth, A.J., 2007. Analysis and functional evaluation of the hair-cell transcriptome. Proc. Natl. Acad. Sci. U. S. A. 104, 11820–11825.

Miyamoto, K., Tatsumi, S., Morimoto, A., Minami, H., Yamamoto, H., Sone, K., Taketani, Y., Nakabou, Y., Oka, T., Takeda, E., 1994. Characterization of the rabbit intestinal fructose transporter (GLUT5). Biochem. J. 303 (Pt 3), 877–883.

Nakazawa, K., Spicer, S.S., Schulte, B.A., 1995. Postnatal expression of the facilitated glucose transporter, GLUT 5, in gerbil outer hair cells. Hear. Res. 82, 93–99.

Pagedar, N.A., Wang, W., Chen, D.H., Davis, R.R., Lopez, I., Wright, C.G., Alagramam, K.N., 2006. Gene expression analysis of distinct populations of cells isolated from mouse and human inner ear FFPE tissue using laser capture microdissection — a technical report based on preliminary findings. Brain Res. 1091, 289–299.

Peters, L.M., Belyantseva, I.A., Lagziel, A., Battey, J.F., Friedman, T.B., Morell, R.J., 2007. Signatures from tissue-specific MPSS libraries identify transcripts preferentially expressed in the mouse inner ear. Genomics 89, 197–206.

Pompeia, C., Hurle, B., Belyantseva, I.A., Noben-Trauth, K., Beisel, K., Gao, J., Buchoff, P., Wistow, G., Kachar, B., 2004. Gene expression profile of the mouse organ of Corti at the onset of hearing. Genomics 83, 1000–1011.

Robertson, N.G., Khetarpal, U., Gutierrez-Espeleta, G.A., Bieber, F.R., Morton, C.C., 1994. Isolation of novel and known genes from a human fetal cochlear cDNA library using subtractive hybridization and differential screening. Genomics 23, 42–50.

Roche, J.P., Wackym, P.A., Cioffi, J.A., Kwitek, A.E., Erbe, C.B., Popper, P., 2005. In silico analysis of 2085 clones from a normalized rat vestibular periphery 3′ cDNA library. Audiol. Neuro-otol. 10, 310–322.

Santos-Sacchi, J., 1991. Reversible inhibition of voltage-dependent outer hair cell motility and capacitance. J. Neurosci. 11, 3096–3110.

Santos-Sacchi, J., Navarrete, E., 2002. Voltage-dependent changes in specific membrane capacitance caused by prestin, the outer hair cell lateral membrane motor. Pflugers Arch. 444, 99–106.

Sugawara-Yokoo, M., Suzuki, T., Matsuzaki, T., Naruse, T., Takata, K., 1999. Presence of fructose transporter GLUT5 in the S3 proximal tubules in the rat kidney. Kidney Int. 56, 1022–1028.

Wu, X., Gao, J., Zuo, J., 2003. Apoptotic cell death in the organ of Corti and absence of Glut5 in outer hair cells in prestin knock-out mice. ARO midwinter meeting, Daytona, FL.

Wu, X., Gao, J., Guo, Y., Zuo, J., 2004. Hearing threshold elevation precedes hair-cell loss in prestin knockout mice. Brain Res. Mol. Brain Res. 126, 30–37.

Wu, X., Currall, B., Yamashita, T., Parker, L.L., Hallworth, R., Zuo, J., 2007. Prestin–prestin and prestin-GLUT5 interactions in HEK293T cells. Dev. Neurobiol. 67, 483–497.

Zheng, J., Shen, W., He, D.Z., Long, K.B., Madison, L.D., Dallos, P., 2000. Prestin is the motor protein of cochlear outer hair cells. Nature 405, 149–155.